

Content from this work may be used under the terms of the CC BY 3.0 licence (© 2018). Any distribution of this work must maintain attribution to the author(s), title of the work, publisher, and DOI.

# DESIGN OF 4 AMPERE S-BAND LINAC USING SLOTTED IRIS STRUCTURE FOR HOM DAMPING\*

J. Pang<sup>†</sup>, X. He, S. Chen, Institute of Fluid Physics, CAEP, Mianyang, China  
 S. Pei, J. Zhang, H. Shi, Institute of High Energy Physics, CAS, Beijing, China

## Abstract

An S-band LINAC with the operating frequency of 2856 MHz and beam current of 4 A was designed for flash X-ray radiography for hydrodynamic test. The optimization of the parameters of the LINAC was processed to obtain the minimum beam radius and the maximum energy efficiency. For the purpose of reducing the beam orbits offset at the exit of LINAC, a slotted iris accelerating structure would be employed to suppress the transverse Higher Order Modes (HOMs) by cutting four radial slots in the iris to couple the HOMs to SiC loads. In this paper, we present the design of the LINAC and the results of beam dynamic analysis.

## INTRODUCTION

Linear induction accelerators were used in large-size or full-size radiographic hydrodynamic test with dose of hundreds of Rad by accelerating several-kA electron beam to tens of MeV. In addition, small machine, such as pulsed X-ray machine with several hundred kV and anode-pinch diode, was used in small-size hydrodynamic subdivision experiments for dynamic material characteristic study, micro jetting diagnosis, et al. Figure 1 shows a typical layout of flash X-ray radiography system.

In the past twenty years, intense-beam normal conducting RF accelerator has been developed with great achievement due to the development of large collider technology. The CLIC Test Facility, CTF3, has accelerated the beam with current of up to 5A to 150MeV with full beam loading [1-2]. The HOM was damped by using slotted iris constant aperture (SICA) accelerating structures. The 100 MeV/100 kW LINAC, constructed by IHEP and used as a driver of a neutron source in KIPT, Ukraine, has accelerated a beam of 2 A to 100 MeV by using detuning accelerating tubes [3-5].

The great progress in intense-beam linac motivates the compact radiographic facility driven by a 4 A 30 MeV linac, which might be utilized for multi-pulse radiographic with the material planar density of several to tens g/cm<sup>2</sup>. The most considered parameter, FWHM of transverse distribution of electron beam, should be limited less than 1 mm. A radiographic system has been discussed in [6]. Simulation results showed that the exposure dose 1 m away from the target right ahead was about 9.1 R and the X-ray spot sizes were not increased with the increment of the thickness of target material. The results also showed that pulse number was limited up to 8 when using a fixed target

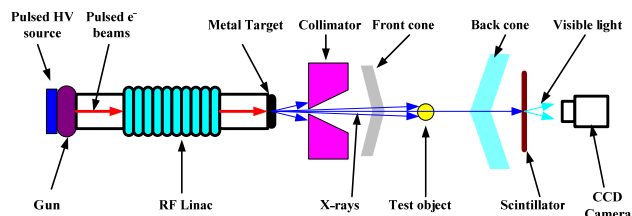


Figure 1: Layout of a typical flash X-ray radiography system using RF accelerator.

when FWHM of transverse size was about 1 mm with bunch charge of 400 nC.

In this paper, the design of accelerator was described. A beam dynamic analysis was carried out with the primary design of the accelerating structure. BBU effect calculation was also carried out.

## GENERAL DESCRIPTION OF THE ACCELERATOR

Layout of the accelerator, which consists of a DC gun, 3 accelerating tube, a chicane and matching beam line, was shown in Fig. 2. The total length is about 14 m and could be reduced by farther optimization. Table 1 lists main parameters.

Table 1: Main Linac Parameters

Parameter	Value	Unit
RF frequency	2856	MHz
Energy	>30	MeV
Beam current (max)	4	A
Energy spread (FWHM)	<0.01	
Emittance (RMS)	<50	mm mrad
Beam pulse length	100	ns
Number of pulses in a train	4-8	
RF pulse duration	10	μs
Pulse repetition rate	10	Hz
Number of ACC. structure	3	
Gun voltage	~120	kV

## ACCELERATING STRUCTURE

### General Design

The goal of the design of accelerating structure is to achieve a high RF-beam power efficiency with short length as much as possible. Two type of structure was considered: the conventional disk-load structure and constant-aperture structure. Both of them should be slotted on the iris to suppress the HOM modes, which would be introduced by

\* Work supported by Key Laboratory of Pulsed Power, CAEP (Contract NO. PPLF2014PZ05) and Key Laboratory of Particle Acceleration Physics & Technology, IHEP, CAS (Contract NO. Y5294109TD)

<sup>†</sup> jpang@caep.cn



Figure 2: Layout of the accelerator.

the beam. The input power, limited by klystron power and transmission efficiency, was determined as 45 MW. There were 3 rules to determine cell arrangements for constant gradient along the axis when there is no beamloading. These rules were described in Ref. [7]

The arrangement of disk-load structure has only a unique solution in the case of certain input power and average unload gradient. Some results with unloaded gradient of 12 MV/m with the different input power calculation are shown in Fig. 3. With a certain beam load and unloaded gradient, the number of cells required to achieve specific microwave-beam efficiency (90% in evaluation) increased linearly with input power, and the loaded gradient satisfying the above requirements did not change.

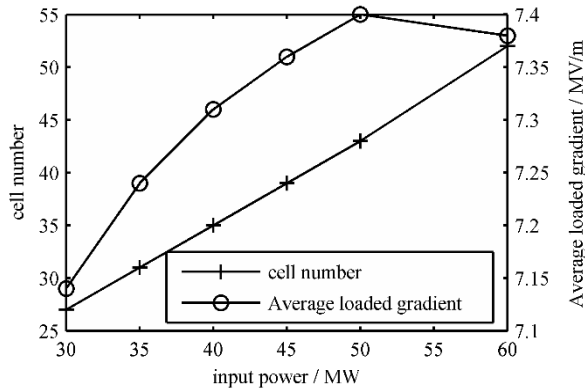


Figure 3: Calculation results of disk-load structure with a certain unloaded gradient of 12 MV/m with various input power.

With the employee of nose cone to achieve constant-aperture, the arrangement is also determined by the iris diameter. With a certain input power, there will be an appropriate value of iris diameter resulting maximum surface electric field as shown in Fig. 4.

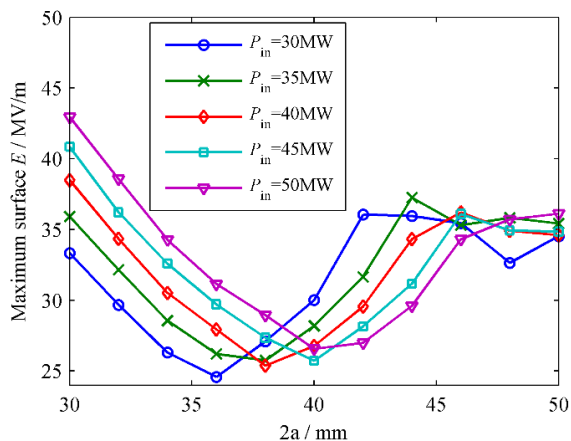


Figure 4: Maximum surface electric field of different structure design.

The designs of two types of structure for 45 MW input power, which are quite similar, are listed in Table 2. The average loaded gradient is larger to CTF3 2998 MHz structure (6.5 MV/m for beam current of 3.5 A [1]), but more critical to the RF breakdown threshold with about 6 times larger RF pulse length. The uniform un-loaded gradient design will bring a lower surface electric field of whole accelerating structure. We chose the disk-load type for our further design.

Table 2: Design of Two Type Accelerating Structures

Parameter	Unit	Disk-load	Constant-aperture
Input power	MW	45	45
$E_{acc}$ (no beamloading)	MV/m	12.0	12.1
$E_{acc}$ (max beamloading)	MV/m	7.36	7.38
$E_{max}$ on surface	MV/m	27.66	29.70
Phase advance per cell		$2\pi/3$ - mode	
RF-beam efficiency		0.893	0.895
Number of cells		39	39
Iris diameter ( $2a$ )	mm	36.010-35.051	36.000
Length of nose cones	mm	-	0.031-0.706
Ratio of $v_g$ to $c$		0.0558-0.0515	0.0550-0.0504
Energy gain	MeV	9.95	9.98

### HOM Damping Design

Four radial slots were cut in the iris to couple HOMs to outer waveguides, where the HOMs would be dissipated in SiC loads. Simulation results shown the frequency and  $Q_0$  of fundamental mode would not be affected by cutting slots with width less than 5 mm.

After cutting slots, the number of dipole modes with frequency below 10GHz of 1<sup>st</sup> cell has increased from about 10 to about 60. Most modes are trapped in ridge waveguides. Important modes have been inherited with large kick factors. Those modes could be considerably damped by using SiC loads, with dielectric constant and tangent delta as 23 and 0.2, relatively, which are quite feasible. The slot width was chosen carefully to minimize BBU effect. The final decision was 3 mm. Beam orbits dispersion simulation was described later in this paper.

The slotted iris would bring a considerable enhancement of surface electric field of fundamental mode in the area near the slot and the center of iris. With a blending radius as 0.3 mm, the enhancement factor would be reduced to about 1.6. When the blending radius was less than 0.2, the calculation of enhancement factor became non-convergent.

Content from this work may be used under the terms of the CC BY 3.0 licence (© 2018). Any distribution of this work must maintain attribution to the author(s), title of the work, publisher, and DOI.

## Test Prototype Tube

A 6-cell prototype tube has been manufactured to test the SiC-copper connecting technique. Six cells were stacked and brazed together without input and output couplers. No crack or detachment of SiC had been found. We are planning to manufacture another prototype tube, which consist of 6 cells and two power couplers, to test our design by high-power conditioning. The double-coupling design would be used to minimum the dipole kick at the entrance of the tube.

## BEAM DYNAMIC

Beam dynamic analysis was carried out using PARMELA code without consideration of BBU. The FWHM of beam horizontal distribution at the end of the accelerator can be controlled less than 1 mm in the case of the 4 A beam load. Figure 5 shows the beam envelop along z axis. Figure 6 shows beam transverse distribution.

If the BBU effect was taken into account, the beam lateral size jitter will be in the order of mm without HOM damping. +200  $\mu\text{m}$ /+200  $\mu\text{rad}$  initial beam offset and angle were assumed at the exit of the buncher and orbit correction were considered.

Calculation results shown that the beam position jitter can be controlled quite well with HOM damping. Figure 7 shows beam orbits dispersion along the accelerating axis with shot width as 1 mm (left) and 3 mm (right). With a 3-mm slot width, the acc. structure shows a better performance of BBU inhibiting, which was shown more clearly in Figure 8. At the exit of accelerator, there were 98% of bunches limited in  $\pm 0.02$  mm beam position jitter when slot width is 3 mm, comparatively, 94% of bunches in  $\pm 0.1$  mm range when slot width is 1 mm.

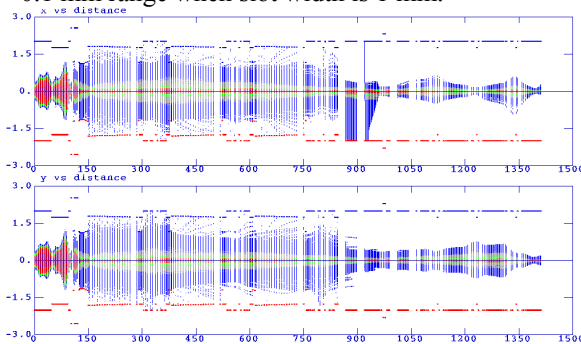


Figure 5: Beam envelope calculation result.

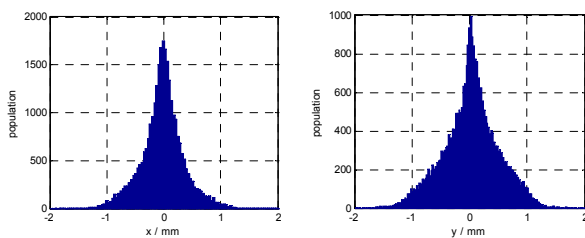


Figure 6: Beam transverse distribution at the exit.

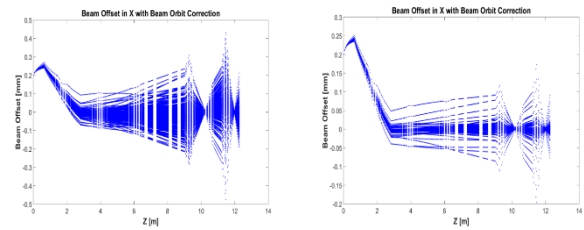


Figure 7: Simulation results of horizontal beam orbits dispersion along the accelerating axis with a 200ns RF duration (including RF fill-up time) considering long-range wakefield with shot width of accelerator structures as 1 mm (left) and 3 mm (right).

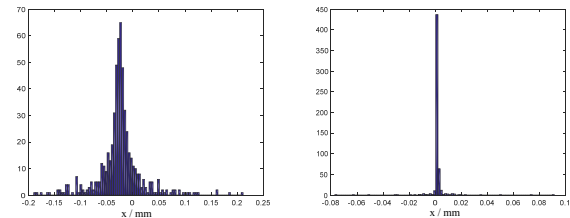


Figure 8: Horizontal distribution of beam orbits dispersion at the exit with shot width of accelerator structures as 1 mm (left) and 3 mm (right).

## REFERENCES

- [1] P. Urschütz *et al.*, “Efficient long-pulse fully loaded CTF3 LINAC operation”, in *Proc. LINAC’2006*, Knoxville, Tennessee, USA, 2006, paper MOP002, pp. 31-33.
- [2] M. Aicheler *et al.*, “A Multi-TeV linear collider based on CLIC technology: CLIC Conceptual Design Report”, CERN, Geneva, Switzerland, Rep. CERN-2012-007, Oct. 2012.
- [3] Y. Chi *et al.*, “Design studies on 100MeV/100kW electron linac for NSC KIPT neutron source on the base of subcritical assembly driven by LINAC”, in *Proc. 2nd Int. Particle Accelerator Conf. (IPAC’11)*, San Sebastián, Spain, 2011, paper TUPC034, pp. 1075-1077.
- [4] M. Aizatskiy *et al.*, “100 MeV/100 kW electron linear accelerator driver of the NSC KIPT neutron source”, in *Proc. 4th Int. Particle Accelerator Conf. (IPAC’13)*, Shanghai, China, 2013, paper THOAB203, pp. 3121-3123.
- [5] S. Pei, private communication, May. 2017.
- [6] J. Pang *et al.*, “Analysis of bremsstrahlung characteristic by 30 MeV multi-pulse beams bombarding rotated tantalum-based target”, *High power laser and particle beams*, vol. 29, no. 6, p. 065101, Jun. 2017.
- [7] J. Pang *et al.*, “Primary Design of 4 A S-band LINAC using slotted iris structure for HOM damping”, in *Proc. The 13th Symposium on Accelerator Physics (SAP’2017)*, Jishou, China, 2017, paper MOPH22, pp.76-78.